Articles

Communication between the Nucleotide Site and the Main Molecular Hinge of 3-Phosphoglycerate Kinase[†]

Judit Szabó,[‡] Andrea Varga,[‡] Beáta Flachner,[‡] Peter V. Konarev,[§] Dmitri I. Svergun,[§] Péter Závodszky,[‡] and Mária Vas*,[‡]

Institute of Enzymology, Biological Research Center, Hungarian Academy of Sciences, H-1518 Budapest, P.O. Box 7, Hungary, EMBL Outstation, c/o DESY, Notkestrasse 85, 22603 Hamburg, Germany, and Institute of Crystallography, Russian Academy of Sciences, Leninsky pr. 59, 117333 Moscow, Russia

Received March 10, 2008; Revised Manuscript Received April 25, 2008

ABSTRACT: 3-Phosphoglycerate kinase is a hinge-bending enzyme with substrate-assisted domain closure. However, the closure mechanism has not been described in terms of structural details. Here we present experimental evidence of the participation of individual substrate binding side chains in the operation of the main hinge which is distant from the substrate binding sites. The combined mutational, kinetic, and structural (DSC and SAXS) data for human 3-phosphoglycerate kinase have shown that catalytic residue R38, which also binds the substrate 3-phosphoglycerate, is essential in inducing domain closure. Similarly, residues K219, N336, and E343 which interact with the nucleotide substrates are involved in the process of domain closure. The other catalytic residue, K215, covers a large distance during catalysis but has no direct role in domain closure. The transmission path of the nucleotide effect toward the main hinge of PGK is described for the first time at the level of interactions existing in the tertiary structure.

Domain movement is the most spectacular phenomenon of protein flexibility and is essential for the function of most multidomain proteins, including enzymes (cf. reviews *1–3*). *Domain closure is generally regulated by sophisticated molecular mechanisms, descriptions of which are required to fully understand the structure−function relationship of multidomain proteins. 3-Phosphoglycerate kinase (PGK)*[1] is the subject of this investigation and is a typical hinge-bending enzyme with two interacting structural domains. PGK catalyzes the phospho transfer from 1,3-bisphosphoglycerate (1,3-BPG) to MgADP and produces 3-phosphoglycerate (3-PG) and MgATP during glycolysis. In addition, PGK plays an important role in the phosphorylation of L-nucleoside analogues which are drug molecules against cancer and viral infections (*4, 5*).

The PGK domains are approximately equal in size (*6–8*), and each of them binds one of the two substrates. 3-PG (*9*) and 1,3-BPG interact with the N-terminal domain, while the nucleotide substrates [MgATP (*10*) or MgADP (*11*)] bind to the C-terminal domain (cf. Figure 1A). Two extreme conformations (open and closed) of the structure of PGK (from different sources) are known (*12–15*). In the open structure, the two bound substrates are distant from each other for the reaction to occur. However, upon closure of the domains, the reactive groups of the substrates move together and become correctly oriented for the catalyzed phospho transfer reaction, as suggested in one of the closed crystal structures (*14*). By comparing different pairs of open and closed crystal structures, Szilágyi et al. proposed that β-strand L (located between the two domains) operates as the main hinge of PGK, since the conformation of βL determines the relative position of the two domains (*15*) (Figure 1A). Location of a hinge at βL has been supported with molecular modeling using DynDom[2] (*2, 16, 17*). However, besides βL, the molecular modeling also identified another possible hinge at the C-terminus of helix 7 which connects the two domains.

[†] The financial support of Grants OTKA (T 043446, T 046412, NI 61915, and D 048578) from the Hungarian National Research Fund, Grant GVOP-3.2.1.2004-04 0195/3.0, and the traveling grants for B.F., J.Sz., and A.V. provided by the European Community-Research Infrastructure Action, under FP6 "Structuring the European Research Area Programme" Contract RII3/CT/2004/5060008, is gratefully acknowledged. D.I.S. and P.V.K. acknowledge support from the EU Design Study "SAXIER", Contract 011934.

* To whom correspondence should be addressed: Institute of Enzymology, BRC, Hungarian Academy of Sciences, H-1518 Budapest, P.O. Box 7, Hungary. Telephone: 36 1 279 3152. Fax: 36 1 466 5465. E-mail: vas@enzim.hu.

[‡] Hungarian Academy of Sciences.

[§] EMBL Outstation, c/o DESY, and Russian Academy of Sciences.

[1] Abbreviations: AMP-PNP, β,γ-imidoadenosine 5′-triphosphate; ANS, 1-anilinonaphthalene-8-sulfonic acid; 1,3-BPG, 1,3-bisphosphoglycerate; CD, circular dichroism; DSC, differential scanning calorimetry; DTT, dithiothreitol; GAPDH, D-glyceraldehyde-3-phosphate dehydrogenase (EC 1.2.1.12); G6PDH, glucose-6-phosphate 1-dehydrogenase (EC 1.1.1.49); HK, hexokinase (EC 2.7.1.1); 3-PG, 3-phosphoglycerate; PGK, 3-phospho-D-glycerate kinase or ATP, 3-phospho-D-glycerate 1-phosphotransferase (EC 2.7.2.3); hPGK, human PGK; SAXS, small-angle X-ray scattering; Tb, *Trypanosoma brucei*; Tm, *Thermotoga maritima*; Bs, *Bacillus stearothermophilus*.

[2] See http://www.cmp.uea.ac.uk/dyndom.

10.1021/bi800411w CCC: $40.75 © 2008 American Chemical Society
Published on Web 06/10/2008

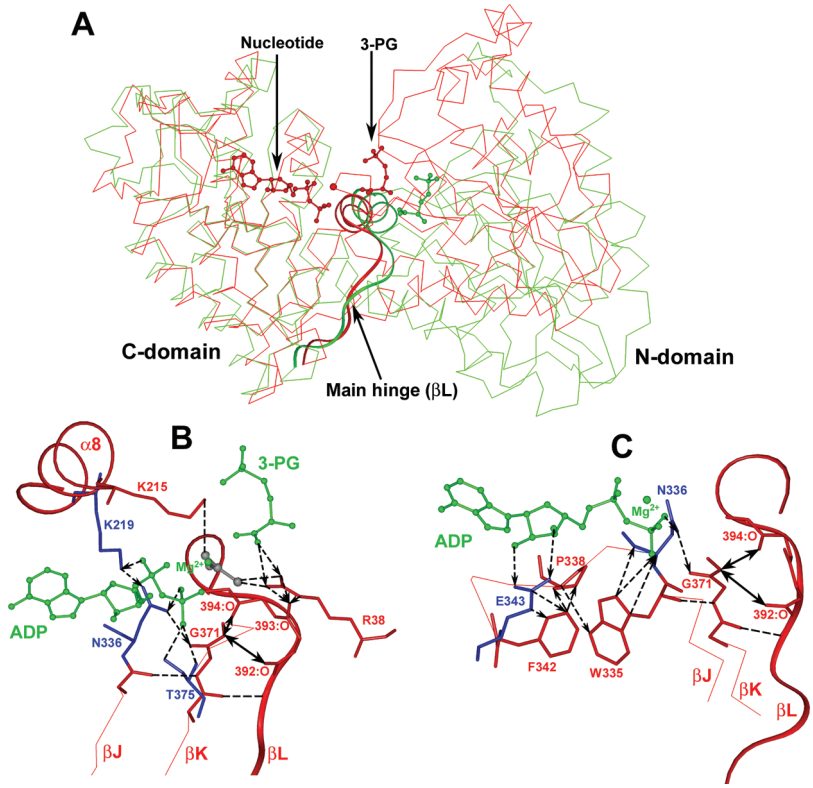

FIGURE 1: β-Strand L operates as the main hinge of PGK. In panel A, the Cα traces of the molecules of the open conformation of the 3-PG binary complex of pig muscle [green (*9*)] and the closed conformation of the MgADP−3-PG ternary complex of *T. brucei* [red, Tb (*14*)] PGKs are superimposed according to the backbone atoms of the core β-sheets of the C-terminal domain. β-Strand L and helix 14 in both structures are highlighted by ribbons. In panels B and C, the structural details (Cα traces, ribbons, and stick models of certain side chains) in the surroundings of the main hinge at βL, including the substrate binding sites, are illustrated in the case of the closed conformation of the MgADP−3-PG ternary complex of *T. brucei* PGK (*14*). In all the panels, 3-PG and the nucleotide are shown as ball-and-stick models. The transferring phospho group is illustrated in panel B as a gray ball-and-stick model. The numbering of the side chains corresponds to the hPGK sequence numbering. The side chains that have been replaced via mutagenesis with Ala are highlighted as blue stick models. The H-bonds and hydrophobic interactions are shown as dashed black lines. Arrows indicate the route of transmission of the effects of 3-PG and the nucleotide toward βL. The H-bonds formed upon domain closure in the ternary complexes are indicated by black double-sided arrows.

From comparison of open and closed crystal structures, hinges at C- and N-termini of helix 7 have also been suggested (*15, 18*). However, analysis of the sequence composition of the termini of helix 7 and the scrutinized atomic contacts of this region excluded the possibility that either of these hinges acts as the main one (*19*).

In contrast, analysis of the atomic contacts of the conserved side chains (which change upon substrate binding) at and in the region of βL suggests that it is plausible that the shape of βL is regulated under the simultaneous action of both substrates. The other hinges at the termini of helix 7 possibly act concertedly with βL due to their direct (through E192 of helix 7) or indirect contacts (*15*). Thus, for operation of the molecular hinge at βL, we have proposed the hypothesis that both substrates together promote domain closure by inducing formation of a double-sided H-bond network around βL (*20*). To test this hypothesis, we have selected conserved residues of human PGK (hPGK) for mutational studies at and near the substrate binding sites, the atomic contacts of which are different in the absence and presence of substrates. Such residues are R38 in the 3-PG binding site and K215, K219, N336, T375, and E343 at the nucleotide site. We have replaced them individually with alanine, and the mutants have been tested in functional (substrate binding and kinetics) as well as structural (DSC and SAXS) investigations. Among the mutants, R38A (*21*) and K215A (*22*) have been characterized in previous functional studies and found to be essential catalytic residues consistent with the structural data. Figure 1B illustrates stabilization of the modeled transferring phospho group by R38 and K215 in the closed active site. Upon domain closure, both local (2−3 Å) and long-range (10 Å) movements of R38 and K215, respectively, have been observed. These observed movements raised the possibility that these catalytic residues participate in domain closure, which is a question that was also addressed.

The results described here demonstrate the important role of R38, but not of K215 (i.e., only one of the two known catalytic residues), in domain movement during catalysis. Moreover, these results also allow us to conclude that among the nucleotide binding residues K219, N336, and E343 contribute to the transmission of the nucleotide effect toward the main hinge, while T375 seems to be irrelevant in this respect. From structural analysis and the mutagenesis studies described here, a detailed description of the possible transmission of this conformational signal is given.

MATERIALS AND METHODS

Chemicals. Na salts of 3-PG, ATP, and ADP were from Boehringer. Substrates MgATP and MgADP were formed by addition of $MgCl_2$ (Sigma) to ATP and ADP, respectively. The dissociation constants of MgATP and MgADP were

taken to be 0.1 and 0.6 mM, respectively (*23–25*). NADH, NADP, and glucose were from Sigma. 1,3-BPG was prepared from glyceraldehyde 3-phosphate (Sigma) according to the Negelein method (*26*) with the modifications described by Furfine et al. (*27*). Isopropyl β-D-thiogalactopyranoside (Fermentas), chloramphenicol, and ampicillin (Sigma) were used for the fermentation. The QuikChange mutagenesis kit was purchased from Stratagene. Primers were produced by Invitrogen. The 1-anilino-8-naphthalenesulfonate (ANS) was purchased from Sigma. All other chemicals were reagent grade commercial preparations.

Enzymes. Expression and purification of recombinant hPGK have been described previously (*22*). The protein solution [20 mg/mL, in a buffer of 50 mM Tris (pH 7.5) containing 1 mM EDTA and 1 mM DTT] was stored at −80 °C. The concentration of the hPGK solution was determined at 280 nm using an extinction coefficient of 27960 M^{-1} cm^{-1} calculated on the basis of a published formula (*28*). Glyceraldehyde-3-phosphate dehydrogenase (GAPDH) was prepared from pig muscle and stored as a microcrystalline suspension (*29*). Hexokinase (HK) and glucose-6-phosphate dehydrogenase (G6PDH) were from Sigma. Solutions of the auxiliary enzymes were dialyzed against the buffer given above.

Site-Directed Mutagenesis. Preparation of R38A and K215A mutants was described previously (*22*). The side chains of K219, N336, E343, and T375 of hPGK were mutated into alanine using the QuikChange site-directed mutagenesis kit (Stratagene). The primers were as follows: K219A, forward (5′-GCTAAAGTTGCAGAC**GCG**ATCCAGCTCATC-3′) and reverse (5′-GATGAGCTGGAT**CGC**GTCTGCAACTTTAGC-3′); N336A, forward (5′-GCAGATTGTGTGG**GCT**GGTCCTGTGGGGG-3′) and reverse (5′-CCCCCACAGGACC**AGC**CCACACAATCTGC-3′); E343A, forward (5′-GTCCTGTGGGGGTATTT**GCA**TGGGAAGCTTTTGCCCG-3′) and reverse (5′-CGGGCAAAAGCTTCCCA**TGC**AAATACCCCCACAGGAC-3′); T375A, forward (5′-GGTGGTGGAGAC**GCT**GCCACTTGCTGTG-3′) and reverse (5′-CACAGCAAGTGGC**AGC**GTCTCCACCACC-3′). The mutations were checked by DNA sequencing.

Circular Dichroism (CD) Spectroscopy. The measurements were carried out with a Jasco 720 spectropolarimeter in the far-UV (200−260 nm) and in the near-UV (260−350 nm) regions. The spectra were measured at 20 °C in 50 mM Tris-HCl buffer containing 1 mM EDTA (pH 7.5), using 0.1 and 1 cm path length cells, at protein concentrations of 0.4 and 2.5 mg/mL (0.009 and 0.056 mM), respectively.

Differential Scanning Calorimetry (DSC) Experiments. The measurements were carried out in a MicroCal VP-DSC-type microcalorimeter (MicroCal Inc.) with a cell volume of 0.51 mL, at a constant scan rate of 60 °C/h in 50 mM Tris-HCl buffer (pH 7.5) containing 1 mM EDTA and 10 mM DTT. For all DSC experiments, samples were degassed and a protein concentration of 0.13 mg/mL (0.003 mM) was used. Although the temperature coefficient of Tris buffer [+0.028 pH/°C (*30*)] is not negligible, the change in pH (from 7.5 to 8.6) during the DSC runs did not affect the results, since neither the activity nor the conformational stability of PGK is changed between pH 7.5 and 8.6 (*31*). The data were analyzed using MicroCal Origin 5.0.

Enzyme Kinetic Studies. The activity of hPGK was measured in both directions of the enzyme reaction with the substrates being either 3-PG and MgATP or 1,3-BPG and MgADP. Both methods and the respective kinetic analyses of the substrate concentration dependencies are described in detail by Flachner et al. (*22*). Briefly, for analysis, besides the well-known Michaelis−Menten equation (applied for all mutants), for wild-type PGK the equation (cf. the Supporting Information) elaborated earlier for the case of activation by the excess of substrate (*32*) has been used. Similarly, anion activation and inhibition of the wild-type enzyme, in the presence of pyrophosphate, were analyzed as described in ref *22*, and the respective equation is shown in the Supporting Information. All the kinetic experiments were carried out at 20 °C in 20 mM Tris-HCl buffer (pH 7.5) containing 1 mM DTT. This buffer ensured the low ionic strength required for studies of the effect of low concentrations of anions.

Substrate Binding Studies: Fluorescence Titrations of hPGK in the Presence of ANS. Fluorescence emission of ANS (fluorescence dye) bound to PGK was detected using a SPEX Fluoromax-3 spectrofluorometer equipped with a Peltier (Edison, NJ) thermostat. The samples were excited at 350 nm using 1 cm path lengths for excitation and 4 mm for emission, and 2 or 4 nm bandwidths were used for excitation; in all cases, 4 nm was applied for emission. The protein and the ANS concentrations were 3 and 150 μM, respectively. The measurements were carried out in 50 mM Tris-HCl and 1 mM EDTA (pH 7.5) at 20 °C. Upon addition of substrates or ligands to the ANS-labeled PGK, characteristic changes in the emitted fluorescence signal (*33*) were used to detect ligand binding and to determine their K_d values for the various enzyme forms. From the measured fluorescence intensity ($F_{measured}$) at a constant wavelength at various concentrations of a given ligand ([L]), the values of K_d were obtained by fitting the experimental points to eqs 1 and 2. For the decrease or increase in the magnitude of the fluorescent signal upon ligand binding:

$$F_{measured} = F_{max} - \frac{(F_{max} - F_{min})[L]}{K_d + [L]} \quad (1)$$

$$F_{measured} = \frac{(F_{max} - F_{min})[L]}{K_d + [L]} \quad (2)$$

It was previously verified that this method gives K_d values comparable to those determined by either the more direct equilibrium dialysis (*34, 35*) or isothermal titration calorimetry (*10*).

Calculation of Thermodynamic Parameters from the Kinetic and Binding Data. The change in Gibbs free energy that accompanies substrate binding (ΔG_S) has been calculated for each substrate from their respective binding constants (K_d) using the known thermodynamic relationship (cf. the Supporting Information).

To express the total activation free energy change ($\Delta G^{\ddagger}_T$) that accompanies the catalytic cycle, we have used the terminology introduced by Fersht (*36*), and the details of the calculations are given in the Supporting Information.

To express the activation free energy change for the chemical step ($\Delta G^{\ddagger}$) of the reaction, the rationale described in the Supporting Information has been applied. The $\Delta G^{\ddagger}$ values were calculated independently from the determined kinetic constants for both of the two randomly bound

substrates and were, as expected, found to be similar to each other. Since the difference between the two values obtained could possibly be due to experimental error, we took the average of these two quantities to characterize the energy requirement of the catalysis in one direction of the enzyme reaction. The analysis was carried out in both the forward and reverse directions of catalysis, for wild-type PGK as well as for its mutants. The thermodynamic parameters are summarized in Table 1 of the Supporting Information.

Small Angle X-ray Scattering (SAXS) Measurements and Data Processing. Synchrotron radiation X-ray scattering data were collected on beamline X33 at the Hamburg EMBL Outstation (*37*) as described by Varga et al. (*20*). Solutions of hPGK (5−15 mg/mL; i.e., 0.1−0.3 mM in storage buffer) and its mutants, as well as its ternary complexes with 3-PG and MgATP in 50 mM Tris-HCl buffer (pH 7.5) containing 1 mM DTT and 1 mM EDTA, were assessed at 20 °C. For all SAXS data, a MAR345 Image Plate at a sample−detector distance of 2.4 m and an X-ray wavelength of 1.5 Å were used, covering the momentum transfer range (s) of 0.012−0.45 Å^{-1} [$s = 4\pi \sin(\theta)/\lambda$, where 2θ is the scattering angle]. To check for radiation damage, the data were collected in two 2 min exposures. These measurements indicated no changes in the scattering patterns with increased exposure time, demonstrating no measurable radiation damage. The data were averaged after normalization to the intensity of the incident beam, and the scattering of the buffer was subtracted. All data manipulations were performed using PRIMUS (*38*). The radii of gyration and the scattering patterns from the crystallographic models of wild-type substrate-free PGK and its various complexes with substrates were computed using CRYSOL (*39*). Computational details for this program are given in the Supporting Information.

Molecular Graphical Analysis. For visualizing and analyzing the molecular details of the hinge region of the closed PGK conformations, Insight II (Biosym/MSI, San Diego, CA) was used. The Protein Data Bank (PDB) codes of the protein coordinates used in structural comparisons are 13PK [*T. brucei* PGK−3-PG−MgADP (*14*)], 1VPE [*Th. maritima* PGK−3-PG−MgAMP-PNP (*12*)], and 1PHP [*B. stearothermophilus* PGK−MgADP (*11*)]. The PDB coordinates of pig muscle PGK−3-PG binary (*9*) and pig muscle PGK−3-PG−MnAMP-PNP ternary (*13*) complexes were obtained from the authors. The limiting values for H-bond, hydrophobic, and ionic interactions are considered to be 3.5, 4.5, and 4.0 Å, respectively.

RESULTS AND DISCUSSION

Effects of Mutations on Substrate Binding by hPGK. To determine the contribution of residues K219, N336, E343, and T375 at the nucleotide site to the binding energy of each substrate, the substrate binding properties of hPGK mutants bearing alanines in place of these residues were characterized. The binding constants (K_d) of each substrate are determined as exemplified in Figure 2. Figure 2A shows the characteristic changes in the emitted fluorescence of the enzyme-bound fluorescent dye (ANS) upon addition of each substrate. As noted previously for wild-type pig muscle PGK (*33*), the nucleotide substrate caused a small but well-defined decrease in the fluorescence intensity, while 3-PG caused a relatively large increase. The same type of characteristic spectral change has been detected for wild-type hPGK as well as for its various mutants. Their similar behavior is in accordance with the absence of conformational perturbation upon mutations (cf. below). Panels B and C of Figure 2 show typical titration curves with MgADP and 3-PG, respectively. The calculated K_d values for all four substrates and for all mutants are summarized in Table 1. For comparison, the results obtained previously with the wild-type enzyme as well as for the mutants of the catalytic residues (R38A and K215A) are also shown. As expected, mutations at the nucleotide site had little to no effect on binding of 3-PG or 1,3-BPG to the N-terminal domain. Conversely, the mutations of K219, N336, and E343 at the nucleotide site weaken the binding of both MgATP and MgADP. However, mutation of K215 exclusively weakens MgATP binding but does not affect MgADP binding. Mutation of T375 exclusively weakens MgADP binding but does not affect MgATP binding. These latter observations are in agreement with the known crystal structures of the binary complexes of PGK with MgADP (*11*) and MgATP (*10*). The X-ray structures revealed interaction of K219 with the α-phosphate of both MgADP and MgATP, while interaction of neither K215 with MgADP nor T375 with MgATP was seen.

Effects of Mutations on the Kinetic Parameters of hPGK. With regard to the kinetic parameters, the k_{cat} values for all mutants (except T375A) are drastically decreased and the K_m values for all substrates are greatly increased. It is also notable that the mutants do not exhibit the peculiar kinetic properties of wild-type PGK, such as activation by the excess of substrates (Figure 1A of the Supporting Information) or by anions (Figure 1B of the Supporting Information). All kinetic results are summarized in Table 1. The disappearance of anion activation upon mutation of residues, such as N336 and E343, having no *a priori* anion binding properties is noticeable. One may assume that this property is closely related to the simultaneous loss of domain closure ability (cf. below), since anion activation and domain closure are interrelated phenomena (*32*).

Among the new mutants, the activity loss is the largest for K219A, and the loss is comparable with the activity decrease caused by mutation of either catalytic residue R38 or K215. This large loss of activity was not expected since in most of the crystal structures, K219 is known to interact with only the α-phosphate of the nucleotide. However, the drastically reduced activity raises the possibility that K219 might also act as a real catalytic residue in concert with K215. NMR (^{19}F) experiments with the transition state analogue AlF_3 are in progress to clarify this point (M. Cliff, personal communication).

The strong influence on the kinetic parameters (both k_{cat} and K_m values) of mutations of N336 and E343 is also remarkable (cf. Table 1). From these data, one can see that the K_m values are generally increased, even in those cases where K_d values are not changed (cf. the K_m values of 3-PG in the case of all the nucleotide site mutants or the K_m value of MgATP in the case of the 3-PG site mutant R38A). From these observations, one can conclude that these side chains assist in formation of the proper interactions of the two substrates in the catalytic Michaelis complex having a closed conformation. Further, when the highly reduced k_{cat} values of N336A and E343A are taken into account, the possibility of a more direct contribution of the side chains of N336 and

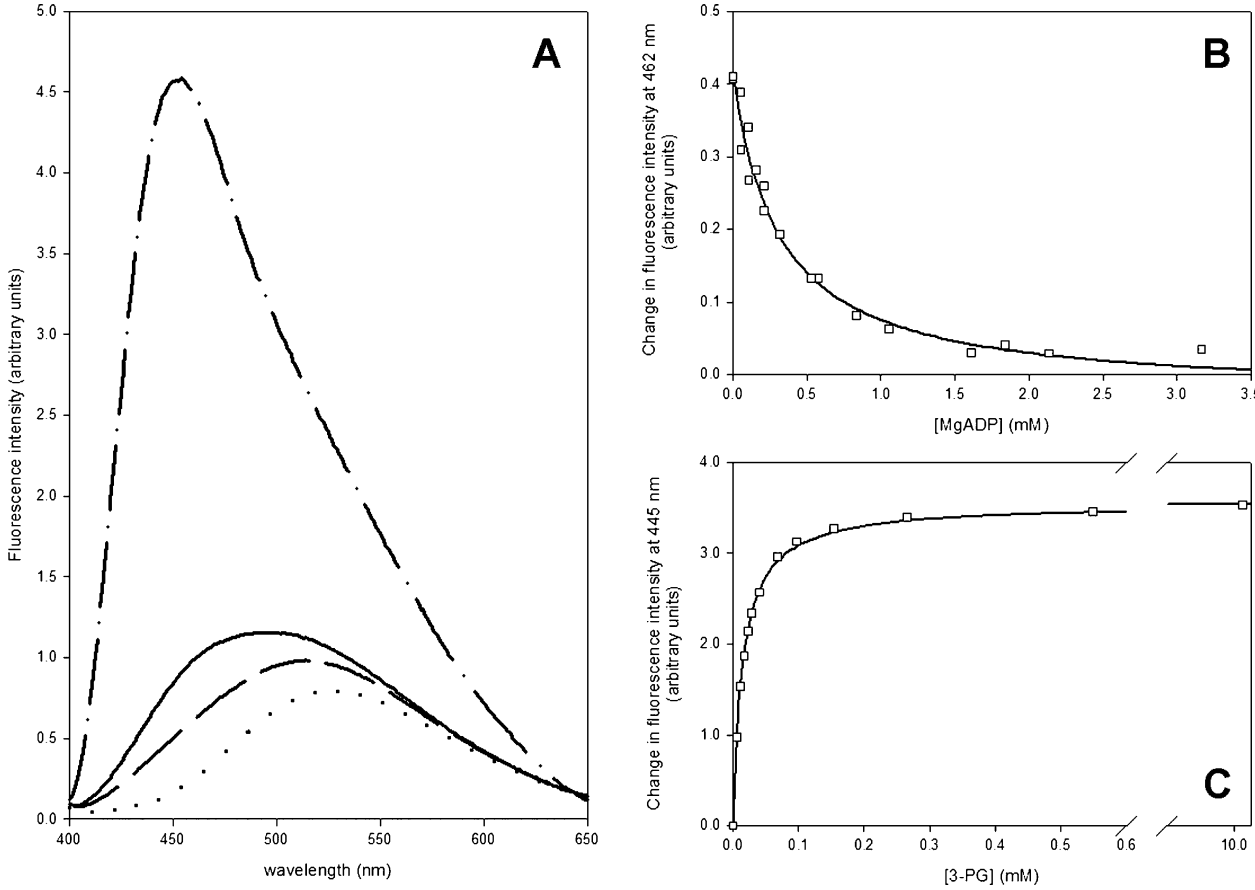

FIGURE 2: Titration of the T375A mutant with substrates using the fluorescence signal of ANS bound to PGK. (A) Fluorescence emission spectra of free ANS (•••) and PGK-bound ANS in the absence of substrates (—) or in the presence of 10 mM ADP and 12.5 mM $MgCl_2$ (– – –) or 10 mM 3-PG (—•—) were recorded as described in Materials and Methods. In panels B and C, the changes of the fluorescence intensity are plotted as a function of the concentration of MgADP and 3-PG, respectively. The solid lines represent the best fit of the experimental data shown in panels B and C to eqs 4 and 5, respectively.

Table 1: Summary of the Functional Properties of Wild-Type and Mutant PGKs[a]

	hPGK[e]	R38A[e]	K215A[e]	K219A	N336A	E343A	T375A
kinetic constants							
reverse direction							
k_{cat} ($v_s a$)	833 ± 50	0.45 ± 0.03	0.48 ± 0.05	0.90 ± 0.07	6.0 ± 0.8	14.3 ± 1.5	125.0 ± 8.3
a (activation factor)	3.8 ± 0.6	1	1	1	1	1	1
K_m^{MgATP}	0.11 ± 0.02	0.96 ± 0.07	2.47 ± 0.2	4.43 ± 0.51	1.34 ± 0.19	1.69 ± 0.06	1.04 ± 0.06
$K_m^{3\text{-PG}}$	0.10 ± 0.02[b] 0.05 ± 0.01[c]	4.5 ± 0.4	0.41 ± 0.04	1.72 ± 0.12	0.54 ± 0.04[d]	0.31 ± 0.03[d]	0.63 ± 0.06
anion activation	+	–	–	–	–	–	–
$K_I^{pyrophosphate}$	0.22 ± 0.07	0.13 ± 0.09	0.51 ± 0.15	0.52 ± 0.11	0.09 ± 0.06	0.14 ± 0.06	1.9 ± 0.6
forward direction							
k_{cat} (V_{max})	2633 ± 417	6.0 ± 0.3	0.78 ± 0.08	5.25 ± 0.83	23.3 ± 1.0	84 ± 2	675 ± 13
K_m^{MgADP}	0.12 ± 0.02	0.10 ± 0.03	0.15 ± 0.03	1.42 ± 0.08	0.42 ± 0.05	0.91 ± 0.11	1.12 ± 0.10
$K_m^{1,3\text{-BPG}}$	(5 ± 2) × 10^{-4}	(2.9 ± 0.1) × 10^{-1}	(3.8 ± 0.3) × 10^{-3}	(7.7 ± 2.2) × 10^{-3}	(2.2 ± 0.8) × 10^{-3}	(1.3 ± 0.2) × 10^{-3}	(3.0 ± 0.8) × 10^{-3}
binding constants							
K_d^{MgATP}	0.33 ± 0.15	0.59 ± 0.20	1.45 ± 0.15	2.65 ± 0.64	1.01 ± 0.22	1.61 ± 0.23	0.22 ± 0.05
K_d^{MgADP}	0.029 ± 0.004	0.035 ± 0.009	0.045 ± 0.007	1.96 ± 0.47	0.38 ± 0.14	0.57 ± 0.10	0.30 ± 0.06
$K_d^{3\text{-PG}}$	0.035 ± 0.008	0.94 ± 0.30	0.039 ± 0.01	0.043 ± 0.001	0.054 ± 0.003	0.032 ± 0.003	0.017 ± 0.005
$K_d^{1,3\text{-BPG}}$	(5.6 ± 2.4) × 10^{-5}	(9.0 ± 2.0) × 10^{-3}	(5.2 ± 1.9) × 10^{-5}	(8.4 ± 1.0) × 10^{-5}	(1.4 ± 0.4) × 10^{-4}	(2.7 ± 0.5) × 10^{-5}	not determined

[a] Rate and equilibrium constants are given in inverse seconds and millimolar, respectively. [b] In the presence of 10 mM MgATP. [c] In the presence of 2.5 mM MgATP. [d] In the presence of 4.0 mM MgATP. [e] Data from ref *22*.

E343 in inducing domain closure is also raised. This possibility is tested below by structural (DSC and SAXS) studies. Among the mutants, T375A affected much more weakly the catalytic efficiency (k_{cat}/K_m) compared to that of wild-type hPGK (cf. Supporting Information, Table 1). Furthermore, this mutation caused a significant weakening of the interaction with the inhibiting anion, pyrophosphate (Table 1). Structural and kinetic studies have suggested the identity of one of the two inhibiting anion sites with the binding site of the nucleotide phosphate(s) in the Michaelis complex (*22*). In agreement, the K_m values for both MgATP and MgADP are significantly increased for the T375A mutant. It follows, therefore, that the side chain of T375 contributes to the formation of the proper catalytic interactions with the nucleotide phosphates.

Energetic Aspects of Mutations in Catalysis. To improve visualization of the effect of mutations on the catalytic parameters, we summarize the values of k_{cat}/K_m together with

the derived activation parameters ($\Delta G_T^{\ddagger}$)[3] of the PGK-catalyzed reaction in Table 1 of the Supporting Information for all the mutants and wild-type hPGK. The table also contains the free energy changes (ΔG_S) of substrate binding derived from the K_d values. The activation free energy changes for the chemical step ($\Delta G^{\ddagger}$) of the enzyme reaction are also listed in this table. Calculation details of these values are described in the Supporting Information. The values for the reaction with 3-PG and MgATP are illustrated in a difference energy diagram ($\Delta\Delta G^{\ddagger}$) for all the mutants, relative to the wild-type enzyme (Figure 3A). This diagram shows the increase in the activation energy of catalysis with different types of mutations. The contribution of the individual mutated side chains to the binding energy of each substrate can also be visualized separately in other difference energy diagrams ($\Delta\Delta G_S$) prepared from ΔG_S data (Figure 3B for 3-PG and Figure 3C for MgATP). It clearly follows from these data that R38 and N336 plus E343 make a considerable contribution to 3-PG and to nucleotide binding, respectively, which is in full agreement with the conclusions described above. Figure 3A clearly supports the closely similar large impacts of the side chains of R38, K215, and K219 on catalysis. Similar conclusions can be also drawn from the equivalent data for the reaction with 1,3-BPG and MgADP (not shown). To better specify the contribution of these side chains to catalysis, we have carried out complementary structural (DSC and SAXS) experiments with the mutants (cf. below). With these methods, the possible role of the side chains in mediation of the large-scale domain movement during the catalytic cycle has been tested.

CD and DSC Studies Elucidate the Effects of Mutations on the Structural Integrity of hPGK. To test whether the mutations introduced have any effect on the structure and stability of the enzyme, CD and DSC measurements were carried out. CD spectra did not indicate any substantial change in the secondary structure of either of the mutants with respect to the wild-type enzyme (some representative spectra are shown in Figure 4A). However, the calorimetric melting curves are more sensitive to even the small extent of changes (as exemplified by Figure 4B). The heat transition curves in all cases indicated cooperative transitions, characteristic of the native fold, and only the melting temperatures were slightly different (Table 2). A significant stabilization (an increase of 5 °C in T_m) upon mutation is observed in the case of N336A, the structural reason for which is unknown.

DSC and SAXS Experiments Elucidate the Effects of Mutations on the Substrate-Caused Domain Closure of hPGK. We have noticed from previous DSC studies that in the ternary complex of the enzyme both substrates together stabilized the PGK conformation better than each of them does separately in the respective binary complexes (*40*). This observation correlated well with the occurrence of domain closure, detected by independent SAXS measurements. Namely, analysis of the SAXS scattering curves has led to the conclusion that simultaneous binding of both substrates is required to induce a domain-closed conformation, which represents the highest-stability form of PGK (*20, 40*). Here we have applied both DSC and SAXS to test the occurrence of domain closure with all nucleotide site mutants, as well as for the R38A mutant, and the results are summarized in Tables 2 and 3. As reported above and previously, R38 is a catalytic residue located in the N-terminal domain (*21, 22*), which participates in the binding of the substrate, 3-PG (*9*) or 1,3-BPG (*14*), and interacts with the transferring phospho group (*14, 22*). At the same time, R38 interacts directly (through the contact with the O atom of T393) with βL

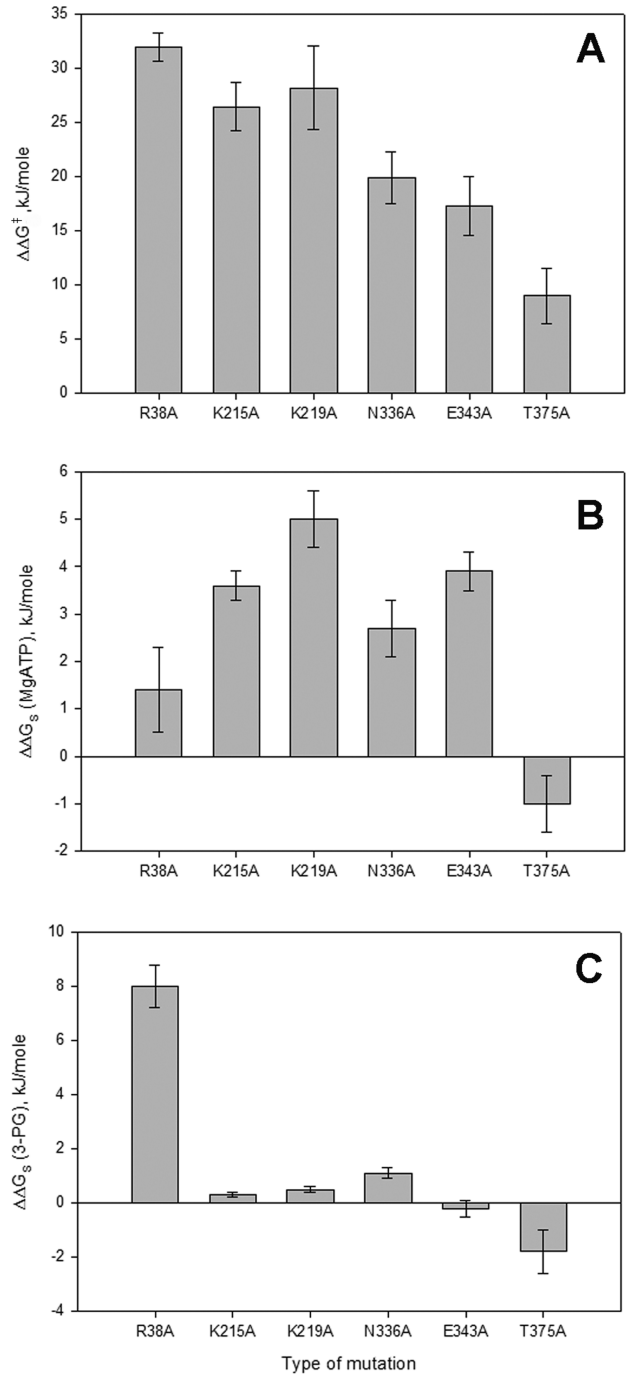

FIGURE 3: Difference energy diagram of the effect of mutations. The activation free energy changes during the reaction catalyzed by the various PGK mutants relative to that of the wild-type enzyme ($\Delta\Delta G^{\ddagger}$) are illustrated in panel A. The free energy changes during MgATP and 3-PG binding by the various mutants relative to wild-type hPGK ($\Delta\Delta G_S$) are shown in panels B and C, respectively. The meaning and the method of calculation of the respective quantities are described in Materials and Methods. The values for both directions of the PGK-catalyzed reactions and for all four substrates are summarized in Table 1 of the Supporting Information.

[3] For the terminology cf. ref *36*.

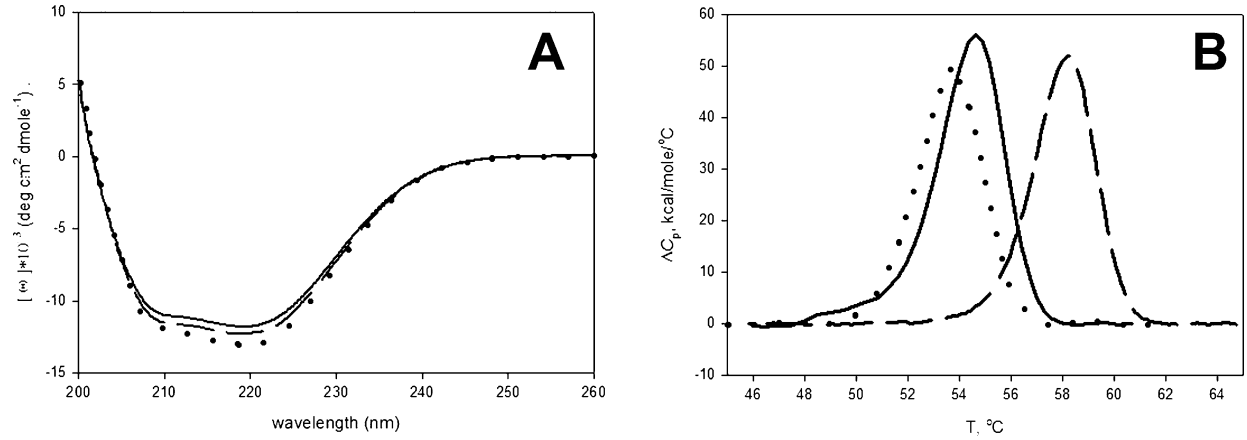

FIGURE 4: Effect of mutations on CD spectra and on the thermal stability of PGK. The far-UV CD spectra (A) and the DSC transition curves (B) of substrate-free wild-type hPGK (—) as well as its mutants, N336A (– – –) and K219A (•••), were recorded. The T_m values together with the results obtained with other mutants as well as those obtained in the presence of substrates are summarized in Table 2.

Table 2: Melting Temperatures (T_m) of Wild-Type and Mutant hPGKs in the Absence and Presence of Saturating Concentrations of Substrates

	T_m (°C)				
	no substrate	with 3-PG	with MgADP	with 3-PG and MgADP	ΔT_m (ternary−binary)[a]
hPGK	54.7	59.1	58.9	60.5	+1.4
K215A	53.5	58.2	57.4	59.2	+1.0
R38A	49.0	50.1	53.8	53.6	−0.2
K219A	53.7	58.4	54.9	57.3	−1.1
N336A	58.2	61.4	59.4	60.9	−0.5
E343A	53.3	58.5	55.9	57.6	−0.9
T375A	53.6	58.1	56.5	58.4	+0.3

[a] ΔT_m values were calculated from the melting temperatures of the ternary minus the more stable binary complexes.

(*12–14; cf. also Figure 1*B); thus, its participation in domain movements is expected and clearly supported by our DSC (Table 2) and SAXS (Table 3) data, suggesting the absence of domain closure for the R38A mutant. Namely, both substrates together in the ternary complex did not improve the stability of the conformation of this mutant compared to the stabilization effect observed in its more stable binary complex with MgADP (Table 2). Furthermore, we have tested the correlation between the experimental SAXS scattering curves of the ternary complex of each mutant (exemplified in Figure 2 of the Supporting Information) and the theoretical curves calculated from various crystal structures (Table 3). Among the X-ray data, the substrate-free enzyme and the binary enzyme−substrate complexes exhibited open conformations, while two ternary complexes of Tm and Tb PGKs exhibited closed conformations. The minimum value of discrepancy (calculated with eq 8 of the Supporting Information and given in bold in Table 3) indicated the best correlation to a given crystal structure. The ternary complex of R38A resembles best that of the open crystal structure. Since R38 interacts with the substrate 3-PG, this finding underlines the importance of this interaction and the 3-PG caused conformational changes in domain closure, the proposal that we have put forward (*20*). Figure 1B illustrates by arrows the transmission of the 3-PG-caused effect toward the main hinge, βL. Similar SAXS experiments revealed that the other catalytic residue, K215, at the nucleotide site does not fill a similar role (cf. Tables 2 and 3). The large-scale movement of this residue during domain closure is possibly dictated by the other residues, K219, N336, and E343, which may be directly involved not only in nucleotide binding but also in domain closure, as suggested by the data presented in Tables 2 and 3. It is seen from the data that the K219A, N336A, and E343A mutants do not exhibit domain closure, even in their ternary complexes with both substrates. On the other hand, T375A exhibits domain closure, indicating that the side chain of T375, although important for the proper interactions with the nucleotide phosphates, has no direct role in the molecular events leading to domain movements.

Molecular Graphical Description of the Communication between the Nucleotide Site and the Hinge. We have proposed that in addition to 3-PG, the nucleotide substrate also participates in inducing the domain-closed conformation: in the active ternary complex the two substrates act together on the main hinge at βL (*20*). Our data clearly demonstrate the importance of K219, N336, and E343 in domain closure. These residues interact with the nucleotide substrates. Panels B and C of Figure 1 depict (by arrows) the possible route of the conformational transmission between the nucleotide site and the main hinge region at βL in the case of the closed Tb PGK crystal structure. In all nucleotide-binding structures, K219/Tb223[4] (located in α-helix 8) and N336/Tb338 (located in βJ) interact with the α- and β-phosphates of the nucleotide, respectively (Figure 1B). Furthermore, K219/Tb223 and N336/Tb338 are also H-bonded to each other. The side chain of N336/Tb338 is H-bonded further to the peptide O atom of G371/Tb374 close to the N-terminus of helix 13. These interactions also strengthen the otherwise existing connections among β-strands J, K, and L; meanwhile, two new H-bonding connections (labeled with double-sided black arrows) are formed between β-strands K and L when both substrates are bound. The formation of the latter two H-bonds leads to an essential change in the conformation of βL, and as a consequence, domain closure is completed.

This structural background clearly supports the role of both nucleotide binding K219 and N336 residues in domain closure. The arrows in Figure 1B designate the pathway of transmission of the nucleotide effect (through the contribution of K219 and N336) toward the hinge at βL. The somewhat smaller activity of K219A compared to that of N336A,

[4] The first and the second numbers refer to hPGK and Tb PGK sequence numbering of the equivalent residue, respectively.

Table 3: Comparison of SAXS Experimental Data with Those Derived from the Crystallographic Models[a]

SAXS experiments			discrepancy values (as given in eq 10) between the scattering from crystallographic models and experimental data					
	R_g(experimental) (Å)[b]		open crystal structures				closed crystal structures	
PGK	GNOM method	Guinier method	pig PGK (no ligand)	Bs PGK−MgADP binary	pig PGK−MgATP binary	pig PGK−3-PG binary	Tm PGK[d] ternary1	Tb PGK[d] ternary2
wild type	22.5 ± 0.5	23.0 ± 0.2	6.14	6.04	4.66	5.31	2.247	**1.61**
R38A	24.0 ± 0.3	24.3 ± 0.3	1.41	1.35	**1.26**	1.33	1.62	1.91
K215A	22.6 ± 0.2	22.9 ± 0.3	3.48	3.74	2.79	2.93	2.26	**2.21**
K219A	23.6 ± 0.4	23.9 ± 0.2	1.49	1.83	1.58	**1.44**	2.32	2.37
N336A	23.7 ± 0.3	24.0 ± 0.2	2.71	3.70	2.89	**2.35**	4.26	3.71
E343A	23.7 ± 0.3	23.9 ± 0.2	1.53	1.75	1.41	**1.37**	1.55	1.66
T375A	22.7 ± 0.3	22.9 ± 0.3	1.92	1.95	1.64	1.69	1.40	**1.37**
R_g(theoretical) (Å)[c]			24.25	24.34	24.02	23.97	23.26	22.64
molecular mass (kDa)[c]			43.7	43.2	43.6	43.8	43.7	45.3

[a] The minimum values of discrepancy (bold) indicate the best correlation between SAXS data and the crystallographic model. Only the ternary complexes exhibit good agreement with the closed crystal structures, while the unliganded PGK and the binary complexes better correlate with the open crystal structures. The small variations in the calculated molecular mass are due to different numbers of residues resolved in different crystal structures. The influence of these variations was checked by deleting appropriate numbers of amino acids from more complete models. These deletions had an only marginal impact on the discrepancy values compared to the opening and closure of the structure, confirming that the small variations in mass did not influence any of the conclusions given above. [b] The experimental R_g values are computed by two alternative methods, using GNOM and the Guinier approximation. [c] The radius of gyration and the molecular mass of the high-resolution models as retrieved from the PDB: PDB entries 1PHP for the Bs PGK−MgADP complex, 1VJC for the pig PGK−MgATP complex, and 1VPE for the Tm PGK ternary and 13PK for Tb PGK ternary complexes. The PDB coordinates of the pig substrate-free structure and the PGK−3-PG binary complex (*9*) were obtained from the authors. [d] ternary1 and ternary2 denote MgAMP-PNP−3-PG and MgADP−3-PG ternary complexes, respectively.

however, raises the question of whether K219 may also have a further role: either it is directly involved in the catalysis (as assumed above), or it may assist in the right positioning of the nucleotide phosphate chain during catalysis. Further studies are needed to answer these questions properly.

As for E343/Tb345, the carboxylate of this residue interacts with the ribose OH groups in all nucleotide binding structures, including *T. brucei* PGK (Figure 1C). The side chain of E343/Tb345 is also involved in the permanent hydrophobic interactions with the sequentially neighboring F342/Tb344, which interacts further with the carbon atoms of the ring of P338/Tb340. This transmission of the nucleotide effect is further continued through the interaction between the rings of P338/Tb340 and W335/Tb337. The latter side chain is contacted further with the main chain carbon and the Cα atoms of Asn336/Tb338. This route is depicted by arrows in Figure 1C. In this way, the effect of the nucleotide is transmitted from both E343 and K219 to the main hinge β-strand L.

General Considerations. Our mutagenesis studies have helped us to uncover in detail the molecular events which are initiated at the substrate sites, are transmitted to the hinge at β-strand L, and finally lead to domain closure. Thus, our results with hPGK are consistent with the involvement of both substrates (each bound to separate domains) in the realization of domain movement during the catalytic cycle. A similar contribution of the substrates, especially of the nucleotides, to the induced fit closure of the active site has been concluded for other kinases, e.g., arginine kinase (*41*) or adenylate kinase (*42, 43*). Our work is entirely consistent with the ligand-driven domain closure model (e.g., ref *43*), which is in apparent contradiction with other literature data (e.g., refs *44* and *45*). We have no experimental data that indicate the occurrence of the conformational transition of PGK in the absence of substrates. However, molecular dynamic simulations indicate the occurrence of domain motion on the time scale of nanoseconds even for substrate-free PGK (*46*). It is indeed possible that the equilibria of these fast conformational fluctuations are perturbed by the bound substrates, which may lead to stabilization of the domain-closed conformations on a much longer time scale.

In the analysis of SAXS data as described above, we classified the scattering patterns on the basis of a series of structures observed in the crystal. Given the potential domain motions in solution, care must be taken when attributing the solution scattering results to a single conformation. It should be noted that the SAXS data alone would not distinguish between a single (e.g., partially closed) state and a mixture of, for example, two extreme (open and closed) states. However, the model of fluctuating protein structure contains not only the two extreme conformations in equilibrium but also many intermediate conformations between them. Substrate binding shifts the equilibrium toward a specific conformation, which would remain the only one observed in the crystal. In solution, multiple fluctuating conformations can be observed, and SAXS reports on the predominant conformation stabilized by the absence or presence of one substrate or both or side chain mutations. Given the existence of partially closed structures in the crystal, mixtures of the two extreme (open and closed) states in solutions can be excluded, but the models best describing the SAXS data should not be considered as rigid conformations of the protein in solution but rather as predominant conformations under the given conditions.

With regard to the energetic (thermodynamic) aspects of domain closure, the question arises about the driving forces required for such a large extent of cooperative motion as domain closure. It is plausible that the binding free energy of substrates can contribute not only to the activation free energy of the chemical step of catalysis but also to the activation free energy of domain closure, which is an inherent event during catalysis. However, the entropic contribution of a protein in its substrate-free form (i.e., internal conformational entropy) to the free energy of substrate binding and the concomitant enzyme catalysis

is less understood. Recent data (*47*) indicate that a close relationship may exist between the total entropy of ligand binding and the internal protein conformational entropy. Thus, the temperature-driven motion may also contribute to the occurrence of domain closure; namely, thermal motions can lead to conformational sampling of protein configurations that facilitate the chemical reactions.

ACKNOWLEDGMENT

The PDB data for substrate-free PGK were provided by Z. Kovári (ELTE, Budapest, Hungary). We thank Adam Round (EMBL Outstation) for his help in preparing the manuscript.

SUPPORTING INFORMATION AVAILABLE

Equations applied in kinetic analyses, calculation of thermodynamic parameters from the enzyme kinetic and binding data, theoretical basis of computation of the SAXS data, summary of the thermodynamic parameters of the substrate binding and catalysis for wild-type and mutant hPGKs (Table 1), effect of mutations on the kinetic properties of hPGK (Figure 1), and SAXS scattering curves of wild-type hPGK as well as of its mutants, R38A and K215A (Figure 2). This material is available free of charge via the Internet at http://pubs.acs.org.

REFERENCES

1. Wriggers, W., and Schulten, K. (1997) Protein domain movements: Detection of rigid domains and visualization of hinges in comparisons of atomic coordinates. *Proteins 29*, 1–14.
2. Hayward, S. (1999) Structural principles governing domain motions in proteins. *Proteins 36*, 425–435.
3. Gerstein, M., and Echols, N. (2004) Exploring the range of protein flexibility, from a structural proteomics perspective. *Curr. Opin. Chem. Biol. 8*, 14–19.
4. Krishnan, P., Gullen, E. A., Lam, W., Dutschman, G. E., Grill, S. P., and Cheng, Y. C. (2003) Novel role of 3-phosphoglycerate kinase, a glycolytic enzyme, in the activation of L-nucleoside analogs, a new class of anticancer and antiviral agents. *J. Biol. Chem. 278*, 36726–36732.
5. Gallois-Montbrun, S., Faraj, A., Seclaman, E., Sommadossi, J. P., Deville-Bonne, D., and Veron, M. (2004) Broad specificity of human phosphoglycerate kinase for antiviral nucleoside analogs. *Biochem. Pharmacol. 68*, 1749–1756.
6. Banks, R. D., Blake, C. C. F., Evans, P. R., Haser, R., Rice, D. W., Hardy, G. W., Merrett, M., and Phillips, A. W. (1979) Sequence, structure and activity of phosphoglycerate kinase: A possible hinge-bending enzyme. *Nature 279*, 773–777.
7. Blake, C. C. F., and Rice, D. W. (1981) Phosphoglycerate kinase. *Philos. Trans. R. Soc. London, Ser. A 293*, 93–104.
8. Watson, H. C., Walker, N. P. C., Shaw, P. J., Bryant, T. N., Wendell, P. L., Fothergill, L., Perkin, R. E., Conroy, S. C., Dobson, M. J., Tuite, M. F., Kingsman, A. J., and Kingsman, S. M. (1982) Sequence and structure of yeast phosphoglycerate kinase. *EMBO J. 1*, 1635–1640.
9. Harlos, K., Vas, M., and Blake, C. C. F. (1992) Crystal structure of the binary complex of pig muscle phosphoglycerate kinase and its substrate 3-phospho-D-glycerate. *Proteins 12*, 133–144.
10. Flachner, B., Kovári, Z., Varga, A., Gugolya, Z., Vonderviszt, F., Náray-Szabó, G., and Vas, M. (2004) Role of Phosphate Chain Mobility of MgATP in Completing the 3-Phosphoglycerate Kinase Catalytic Site: Binding, Kinetic, and Crystallographic Studies with ATP and MgATP. *Biochemistry 43*, 3436–3449.
11. Davies, G. J., Gamblin, S. J., Littlechild, J. A., Dauter, Z., Wilson, K. S., and Watson, H. C. (1994) Structure of the ADP complex of the 3-phosphoglycerate kinase from *Bacillus stearothermophilus* at 1.65 Å. *Acta Crystallogr. D50*, 202–209.
12. Auerbach, G., Huber, R., Grättinger, M., Zaiss, K., Schurig, H., Jaenicke, R., and Jacob, U. (1997) Closed structure of phosphoglycerate kinase from *Thermotoga maritima* reveals the catalytic mechanism and determinants of thermal stability. *Structure 5*, 1475–1483.
13. May, A., Vas, M., Harlos, K., and Blake, C. C. F. (1996) 2.0 Å resolution structure of a ternary complex of pig muscle phosphoglycerate kinase containing 3-phospho-D-glycerate and the nucleotide Mn adenylylimidodiphosphate. *Proteins 24*, 292–303.
14. Bernstein, B. E., and Hol, W. G. (1998) Crystal structures of substrates and products bound to the phosphoglycerate kinase active site reveal the catalytic mechanism. *Biochemistry 37*, 4429–4436.
15. Szilágyi, A. N., Ghosh, M., Garman, E., and Vas, M. (2001) A 1.8 Å resolution structure of pig muscle 3-phosphoglycerate kinase with bound MgADP and 3-phosphoglycerate in open conformation: New insight into the role of the nucleotide in domain closure. *J. Mol. Biol. 306*, 499–511.
16. Hayward, S., and Berendsen, H. J. (1998) Systematic analysis of domain motions in proteins from conformational change: New results on citrate synthase and T4 lysozyme. *Proteins 30*, 144–154.
17. Lee, R. A., Razaz, M., and Hayward, S. (2003) The DynDom database of protein domain motions. *Bioinformatics 19*, 1290–1291.
18. Bernstein, B. E., Michels, P. A. M., and Hol, W. G. J. (1997) Synergistic effects of substrate-induced conformational changes in phosphoglycerate kinase activation. *Nature 385*, 275–278.
19. Kovári, Z., and Vas, M. (2004) Protein conformer selection by sequence-dependent packing contacts in crystals of 3-phosphoglycerate kinase. *Proteins 55*, 198–209.
20. Varga, A., Flachner, B., Konarev, P., Gráczer, É., Szabó, J., Svergun, D., Závodszky, P., and Vas, M. (2006) Substrate-induced double sided H-bond network as a means of domain closure in 3-phosphoglycerate kinase. *FEBS Lett. 580*, 2698–2706.
21. Sherman, M. A., Fairbrother, W. J., and Mas, M. T. (1992) Characterization of the structure and properties of the His62→Ala and Arg38→Ala mutants of yeast phosphoglycerate kinase: An investigation of the catalytic and activatory sites by site-directed mutagenesis and NMR. *Protein Sci. 1*, 752–760.
22. Flachner, B., Varga, A., Szabó, J., Barna, L., Hajdú, I., Gyimesi, G., Závodszky, P., and Vas, M. (2005) Substrate-Assisted Movement of the Catalytic Lys 215 during Domain Closure: Site-Directed Mutagenesis Studies of Human 3-Phosphoglycerate Kinase. *Biochemistry 44*, 16853–16865.
23. Larsson-Raznikiewicz, M. (1964) Kinetic studies on the reaction catalysed by phosphoglycerate kinase: I. The effect of Mg^{2+} and adenosine-5′-triphosphate. *Biochim. Biophys. Acta 85*, 60–68.
24. Miller, C., Frey, C. M., and Stuehr, J. E. (1972) Interactions of divalent metal ions with inorganic and nucleotide phosphates. I. Thermodynamics. *J. Am. Chem. Soc. 94*, 8898–8904.
25. Zhang, W., Truttmann, A. C., Luthi, D., and McGuigan, J. A. (1997) Apparent Mg^{2+}-adenosine 5-triphosphate dissociation constant measured with Mg^{2+} macroelectrodes under conditions pertinent to ^{31}P NMR ionized magnesium determinations. *Anal. Biochem. 251*, 246–250.
26. Negelein, E., and Brömel, H. (1939) *Biochem. Z. 301*, 135.
27. Furfine, C. S., and Velick, S. F. (1965) The Acyl-Enzyme Intermediate and the Kinetic Mechanism of the Glyceraldehyde 3-Phosphate Dehydrogenase Reaction. *J. Biol. Chem. 240*, 844–855.
28. Pace, C. N., Vajdos, F., Fee, L., Grimsley, G., and Gray, T. (1995) How to measure and predict the molar absorption coefficient of a protein. *Protein Sci. 4*, 2411–2423.
29. Elõdi, P., and Szörényi, E. (1956) Crystallisation and comparative studies of D-glyceraldehyde-3-phosphate dehydrogenase from muscle of various mammals. *Acta Physiol. Hung. 9*, 339–350.
30. Dawson, R. M. C., Elliott, D. C., Elliott, W. H., and Jones, K. M. (1986) *Data for Biochemical Research*, 3rd ed., pp 426 Oxford University Press, New York.
31. Krietsch, W. K., and Bücher, T. (1970) 3-Phosphoglycerate kinase from rabbit sceletal muscle and yeast. *Eur. J. Biochem. 17*, 568–575.
32. Szilágyi, A. N., and Vas, M. (1998) Anion activation of 3-phosphoglycerate kinase requires domain closure. *Biochemistry 37*, 8551–8563.
33. Vas, M., and Batke, J. (1984) Adenine nucleotides affect the binding of 3-phosphoglycerate to pig muscle 3-phosphoglycerate kinase. *Eur. J. Biochem. 139*, 115–123.
34. Molnár, M., and Vas, M. (1993) Mg^{2+} affects the binding of ADP but not ATP to 3-phosphoglycerate kinase. Correlation between equilibrium dialysis binding and enzyme kinetic data. *Biochem. J. 293*, 595–599.

35. Merli, A., Szilágyi, A. N., Flachner, B., Rossi, G. L., and Vas, M. (2002) Nucleotide Binding to Pig Muscle 3-Phosphoglycerate Kinase in the Crystal and in Solution: Relationship between Substrate Antagonism and Interdomain Communication. *Biochemistry 41*, 111–119.
36. Fersht, A. R. (1999) *Structure and Mechanism in Protein Science: A Guide to Enzyme Catalysis and Protein Folding*, 2nd ed., pp 350−355, Freeman & Co., New York.
37. Roessle, M. W., Klaering, R., Ristau, U., Robrahn, B., Jahn, D., Gehrmann, T., Konarev, P., Round, A., Fiedler, S., Hermes, C., and Svergun, D. (2007) Upgrade of the small-angle X-ray scattering beamline X33 at the European Molecular Biology Laboratory, Hamburg. *J. Appl. Crystallogr. 40*, s190−s194.
38. Konarev, P. V., Volkov, V. V., Petoukhov, M. V., and Svergun, D. I. (2006) ATSAS 2.1, a program package for small-angle scattering data analysis. *J. Appl. Crystallogr. 39*, 277–286.
39. Svergun, D. I., Barberato, C., and Koch, M. H. J. (1995) CRYSOL: A program to evaluate X-ray solution scattering of biological macromolecules from atomic coordinates. *J. Appl. Crystallogr. 28*, 768–773.
40. Varga, A., Flachner, B., Gráczer, E., Osváth, S., Szilágyi, A. N., and Vas, M. (2005) Correlation between conformational stability of the ternary enzyme-substrate complex and domain closure of 3-phosphoglycerate kinase. *FEBS J. 272*, 1867–1885.
41. Yousef, M. S., Clark, S. A., Pruett, P. K., Somasundaram, T., Ellington, W. R., and Chapman, M. S. (2003) Induced fit in guanidino kinases: Comparison of substrate-free and transition state analog structures of arginine kinase. *Protein Sci. 12*, 103–111.
42. Muller, C. W., Schlauderer, G. J., Reinstein, J., and Schulz, G. E. (1996) Adenylate kinase motions during catalysis: An energetic counterweight balancing substrate binding. *Structure 4*, 147–156.
43. Hayward, S. (2004) Identification of specific interactions that drive ligand-induced closure in five enzymes with classic domain movements. *J. Mol. Biol. 339*, 1001–1021.
44. Stillman, T. J., Migueis, A. M., Wang, X. G., Baker, P. J., Britton, K. L., Engel, P. C., and Rice, D. W. (1999) Insights into the mechanism of domain closure and substrate specificity of glutamate dehydrogenase from *Clostridium symbiosum*. *J. Mol. Biol. 285*, 875–885.
45. Henzler-Wildman, K. A., Lei, M., Thai, V., Kerns, S. J., Karplus, M., and Kern, D. (2007) A hierarchy of timescales in protein dynamics is linked to enzyme catalysis. *Nature 450*, 913–916.
46. Balog, E., Laberge, M., and Fidy, J. (2007) The influence of interdomain interactions on the intradomain motions in yeast phosphoglycerate kinase: A molecular dynamics study. *Biophys. J. 92*, 1709–1716.
47. Frederick, K. K., Marlow, M. S., Valentine, K. G., and Wand, A. J. (2007) Conformational entropy in molecular recognition by proteins. *Nature 448*, 325–329.

BI800411W